ISSN 0006-2979, Biochemistry (Moscow), 2024, Vol. 89, No. 10, pp. 1711-1726 © Pleiades Publishing, Ltd., 2024.

Placental Transport of Amino Acids in Rats with Methionine-Induced Hyperhomocysteinemia

Yulia P. Milyutina[1,a]*, Gleb O. Kerkeshko[1], Dmitrii S. Vasilev[1,2], Irina V. Zalozniaia[1], Sergey K. Bochkovskii[1], Natalia L. Tumanova[2], Anastasiia D. Shcherbitskaia[1], Anastasiia V. Mikhel[1], Gulrukhsor H. Tolibova[1], and Alexander V. Arutjunyan[1]

[1]*D. O. Ott Research Institute of Obstetrics, Gynecology, and Reproductive Medicine, 199034 St. Petersburg, Russia*

[2]*I. M. Sechenov Institute of Evolutionary Physiology and Biochemistry, Russian Academy of Sciences, 194223 St. Petersburg, Russia*

[a]*e-mail: milyutina1010@mail.ru*

Received December 2, 2023
Revised April 11, 2024
Accepted May 2, 2024

Abstract—Maternal hyperhomocysteinemia (HHcy) is a risk factor for intrauterine growth restriction presumably caused by a decrease in the placental transport of nutrients. We investigated the effect of experimental HHcy induced by daily methionine administration to pregnant rats on the free amino acid levels in the maternal and fetal blood, as well as on morphological and biochemical parameters associated with the amino acid transport through the placenta. HHcy caused an increase in the levels of most free amino acids in the maternal blood on gestational day 20, while the levels of some amino acids in the fetal blood were decreased. In rats with HHcy, the maternal sinusoids in the placental labyrinth were narrowed, which was accompanied by aggregation of red blood cells. We also observed an increase in the neutral amino acid transporters (LAT1, SNAT2) protein levels and activation of 4E-BP1, a downstream effector of mTORC1 complex, in the labyrinth zone. Maternal HHcy affected the placental barrier permeability, as evidenced by intensification of the mother-to-fetus transfer of Evans Blue dye. The imbalance in the free amino acid levels in the maternal and fetal blood in HHcy may be due to the competition of homocysteine with other amino acids for common transporters, as well as a decrease in the area of exchange zone between maternal and fetal circulations in the placental labyrinth. Upregulation of the neutral amino acid transporter expression in the labyrinth zone may be a compensatory response to an insufficient intrauterine amino acid supply and fetal growth restriction.

DOI: 10.1134/S0006297924100055

Keywords: maternal hyperhomocysteinemia, placenta, placental transport, placental barrier, amino acids, mTOR, amino acid transporters

INTRODUCTION

One of consequences of the elevated content of the non-proteinogenic amino acid homocysteine (Hcy), an intermediate metabolite of methionine, in the mother's blood during pregnancy is fetal growth restriction and reduced birth weight [1-3]. The negative effects of maternal hyperhomocysteinemia (HHcy) on the fetal growth and development likely associated with the toxic effects of high Hcy levels are still poorly understood.

Placenta plays a key role in the regulation of nutrient distribution between mother and fetus during

Abbreviations: 4E-BP1, eukaryotic translation initiation factor 4E-binding protein 1; 5-HT, serotonin; AA, amino acid; FPP, fetal-faced placental part; GD, gestational day; HHcy, hyperhomocysteinemia; Hcy, homocysteine; LAT, L-type amino acid transporter; MPP, maternal-faced placental part; mTOR, mammalian target of rapamycin; mTORC1, mammalian target of rapamycin complex 1; S6, ribosomal protein S6; SNAT, sodium-coupled neutral amino acid transporter; STB, syncytiotrophoblast; TGC, trophoblast giant cell.

* To whom correspondence should be addressed.

pregnancy, as it integrates the signals on the maternal and fetal nutrient availability [4]. The main placental sensor of the nutrient level in the mother's blood is the mTORC1 complex containing mammalian target of rapamycin (mTOR) as a catalytic unit [5, 6]. Maternal nutritional deficiencies, stress, and placental hypoxia result in reduction of the mTORC1 activity in the placenta and cause a corresponding decrease in the expression of placental nutrient transporters [7]. An excess of nutrients in the maternal blood, on the contrary, results in the activation of placental mTORC1 accompanied by an increase in the number of placental transporters [8]. It has been suggested that in addition to signals from the maternal side, the transport function of the placenta is regulated by nutrition status-related signaling from the fetal side, which allows to compensate a decrease in the available nutrients in the fetal blood by increasing expression and activity of placental transporters [7, 9].

An adequate placental transport of amino acids (AAs) from mother to fetus is vital for fetal growth [10]. The rate of AA transport through the placenta is determined by the rate of maternal placental blood flow, surface area of the exchange zone between the maternal and fetal circulations, and activity and number of AA transporters in this zone [10]. In rodents, such an exchange zone and at the same time a placental barrier is a continuous two-layered syncytiotrophoblast (STB) lining sinusoids filled with maternal blood in the labyrinthine region of the placenta. The expression and activity of the neutral AA transporters on the STB membranes are controlled by the mTORC1 complex [11].

Experimental studies have shown that HHcy is accompanied by changes in the free AAs profiles in the blood and cerebral spinal fluid of male mice, as well as in the blood of pregnant rats and brains of their fetuses [12-16]. It has been hypothesized that Hcy can inhibit the mother-to-fetus neutral AA transport by competing with AAs for common transporters on the STB membranes [17, 18], and, consequently, affect the levels of AAs in the maternal and fetal blood. Methionine and, possibly, Hcy are able to change the activity of mTORC1 by modulating the intracellular content of mTORC1 activator S-adenosylmethionine [24, 25]. The studies conducted on brain tissues or neural cells have demonstrated that elevated Hcy levels can influence the mTORC1 activity [19-23]. At the same time, the effect of maternal HHcy on the activity of mTORC1 and levels of AA transporters in the placenta remains poorly studied. No changes in the activity of mTORC1 under the influence of increasing Hcy concentration were observed in primary human trophoblast cells [26]; on the other hand, administration of methionine to animals increases the activity of mTORC1 and upregulated expression of AA transporters in the placental tissues [27, 28].

Thus, HHcy can affect the transport of AAs from mother to fetus via the competition of Hcy with other AAs for common placental transporters, and through the change in the activity of the mTORC1 complex and mTORC1-regulated expression of AA transporters on the STB membranes. On the other hand, due to the presumed existence of fetal feedback, the compensatory increase in the expression and/or activity of placental AA transporters may occur in response to the decreasing of fetal blood AA concentrations and fetal growth retardation. Furthermore, the possibility of direct toxic effects of high Hcy levels on placental cells, which could result in the delay in placental development and the decrease of its transport and barrier function, should be also considered. In order to test these hypotheses, we investigated the effects of methionine-induced HHcy on the free AAs content in the blood of pregnant rats and their fetuses, placental mTORC1 signaling and neutral AA transporters expression in the placental labyrinth, as well as on the morphology of placenta and placental barrier integrity.

MATERIALS AND METHODS

Animals. Female 3 to 4-month-old Wistar rats (n = 33; Rappolovo Animal Facility, Russia) with the initial body weight of 220-290 g and stable estrous cycle of 4 days, were used in the experiments. The animals were housed at the animal facility with a forced ventilation and controlled 12-h light/dark cycle (daytime, 7.00-19.00; nighttime, 19.00-7.00) at a constant temperature of 20-21°C and 75-85% humidity. The rats received a standard feed for laboratory animals (Provimi, Russia) and filtered water *ad libitum*. All experiments were conducted in accordance with the Directive of European Union (86/609/EEC) on protection of animals used in experimental studies.

Model of maternal HHcy. Experimental maternal HHcy was induced by chronic methionine administration to pregnant animals according to the method previously developed in our laboratory [29, 30]. The day after detection of spermatozoa in the vaginal smear was considered as the gestational day 1 (GD1). Pregnant animals were divided into control (n = 15) and experimental (HHcy; n = 18) groups. Experimental animals received daily 1 ml of aqueous solution of L-methionine [AJI92, USP30 (TLC); Khimmed, Russia] prepared *ex tempora*. L-Methionine was administered perorally at 0.6 g/kg of animal body weight via oral gavage from GD4 to GD19. Control animals received 1 ml of water administered the same way for the same period of time.

Evaluation of weight gain in pregnant rats. In order to determine the total weight gain, female rats were weighted prior to mating and on GDs 4, 10,

14, and 20. The obtained data were used to plot the dependence of body weight on the gestation period for each animal. The slopes of the obtained plots were compared for the control and experimental groups. Animals with total number of fetuses between 11 and 16 were included in the analysis. The average number of fetuses in the animals from the control and experimental groups did not differ.

Tissue collection for analysis. Pregnant rats from both groups were sacrificed by decapitation without anesthesia using a guillotine for laboratory rodents (Open Science, Russia) on GD20, 24 h after the last administration of methionine, and their trunk blood was collected. Fetuses and placentas were isolated and weighted. The fetuses were decapitated and their trunk blood was collected (blood from the entire litter of each dam was pooled together). Placentas for histology examination were immediately placed into 10% neutral buffered formalin solution (pH 7.2) (Sintakon, Russia). Blood serum was obtained by centrifugation (10 min at 2300*g*). Blood serum samples and placenta tissues for biochemical analysis were stored at –80°C.

HPLC analysis of the free AAs in the maternal and fetal blood serum was carried out according to the method described by Askretkov et al. [31]. An AccQ-Fluor Reagent Kit (Waters, USA) was used for AA derivatization. Standard solution of the 17 AA (Ala, Arg, Asp, Cystine, Glu, Gly, His, Ile, Leu, Lys, Met, Phe, Pro, Ser, Thr, Tyr, Val) (Waters), individual standard solutions of Asn, Gln, Trp, and internal standard alanyl-glutamine peptide were used. Analysis was carried out with a Dionex Ultimate 3000 HPLC system (Thermo Fisher Scientific, Germany) equipped with an FLD-3100 fluorescence detector. To analyze biological samples, 50 µl of the internal standard and 50 µl of the blood serum were mixed. To precipitate proteins, acetonitrile was added to a sample at a 1 : 1 ratio and the mixture was centrifuged for 5 min at 10,000*g*. An aliquot (10 µl) of the supernatant was mixed in a vial with 70 µl of AccQ-Fluor Borate Buffer (Waters) from the derivatization reagent kit and 20 µl of 10 mM solution of 6-aminoquinoline-N-hyroxysuccineimidyl carbamate (AQC; Waters) in acetonitrile; the mixture was incubated for 1 min at room temperature and then for 10 min at 50°C. The vials were placed into an autosampler of the chromatograph and AAs were separated on a reversed-phase AccQ-Tag column (3.9 × 150 mm; particle size, 4 µm; Waters) in a gradient mode at a mobile phase flow rate of 1 ml/min (injected sample volume, 2 µl; column temperature, 37°C). Detection was carried out based on the fluorescence intensity at 395 nm (λ_{ex} = 250 nm). The obtained chromatograms were processed using the Chromeleon 7.0 chromatography data system (Thermo Scientific, USA) and Microsoft Office Excel. The content of the following 17 individual AA in maternal and fetal serum was determined: His, Ile, Leu, Lys, Met, Phe, Thr, Trp, Val, Asn, Asp, Gln, Glu, Gly, Ser, Tyr, and Pro (the method used did not allow separate quantification of Ala and Arg, hence, a combined content Ala + Arg was determined). The ratio of fetal blood content to maternal blood content for each AA was also calculated.

Immunoblotting was used to investigate the effect of maternal HHcy on the content of neutral AA transporters in the placenta and on the activation of signaling pathways controlled by the mTORC1 complex. One placenta from each dam in the group was used for analysis. Prior to analysis, frozen placenta tissues were washed from blood with cold 10 mM phosphate buffer (pH 7.4) and separated into two parts: maternal-faced placental part (MPP) including the basal zone (spongiotrophoblast) with thin layer of decidua basalis, and fetal-faced placental part (FPP) containing the labyrinth zone. Placental tissues were homogenized with a glass Dounce homogenizer at a 1 : 2 (*w/v*) ratio in RIPA buffer [50 mM Tris-HCl (pH 8.1), 1% Triton X-100, 0.1% sodium dodecyl sulfate (SDS), 0.5% sodium deoxycholate, 1 mM EDTA, 150 mM NaCl] supplemented with a protease inhibitor cocktail (S8820; Sigma-Aldrich) and phosphatase inhibitor cocktail (P5726; Sigma-Aldrich) and centrifuged for 20 min at 16,000*g* and 4°C; the resulting supernatant was used for analysis. Total protein concentration in the samples was determined using Bradford protein assay [32] with a NanoDrop One spectrophotometer (Thermo Scientific). The samples (50 µg of protein) were separated by electrophoresis in 10% PAAG under denaturing condition according to the Laemmli procedure in a Mini-Protean Tetra Cell (Bio-Rad, USA) with a PowerPac HC power source (Bio-Rad) and transferred onto a PVDF membrane (Bio-Rad) in a semi-dry Trans-Blot Turbo Transfer System (Bio-Rad). The membranes were blocked with 3% bovine serum albumin (Sigma-Aldrich) in TBST buffer [50 mM Tris-HCl; 150 mM NaCl; 0.1% (*v/v*) Tween 20; pH 7.5] and incubated overnight at 4°C with the specific primary antibodies against SNAT1 [SNAT1 (H-9) mouse mAb; sc-137032, Santa Cruz Biotechnology, USA; 1 : 1000] (55 kDa); SNAT2 [SNAT2 (G-8) mouse mAb; sc-166366, Santa Cruz Biotechnology; 1 : 1000] (60 kDa); LAT1 [LAT1 (D-10) mouse mAb, sc-374232, Santa Cruz Biotechnology; 1 : 1000] (45 kDa); LAT2 [LAT2 Rabbit Ab, ab75610, Abcam, UK; 1 : 1000] (58 kDa); mTOR [mTOR (7C10) rabbit mAb, 2983S, Cell Signaling, USA; 1 : 1000] (289 kDa); phospho-mTOR [phospho-mTOR (Ser2448) rabbit Ab, 2971S, Cell Signaling; 1 : 1000] (289 kDa); 4E-BP1 [4E-BP1 (53H11) rabbit mAb, 9644S, Cell Signaling; 1 : 1000] (15-20 kDa); phospho-4E-BP1 [phospho-4E-BP1 (Thr37/46) (236B4) rabbit mAb, 2855S, Cell Signaling; 1 : 1000] (15-20 kDa); S6 [S6 ribosomal protein (5G10) rabbit mAb, 2217S, Cell Signaling; 1 : 1000] (32 kDa); and phospho-S6 [phospho-S6 ribosomal protein (Ser235/236) (D57.2.2E) rabbit mAb, 4858S,

Cell Signaling; 1 : 1000] (32 kDa). Next, the membranes were incubated with the corresponding secondary goat antibodies conjugated with horseradish peroxidase (HRP) (1 : 1000; Bio-Rad), and the proteins were visualized using a Clarity Western ECL Substrate (Bio-Rad). The membranes were scanned with a ChemiDoc™ Touch Imaging system (Bio-Rad); the band intensity was determined with the ImageLab 5.2.1 software. The obtained data were normalized either to the level of glyceraldehyde 3-phosphate dehydrogenase (GAPDH) [GAPDH (14C10) rabbit mAb, 2118S, Cell Signaling; 1 : 1000) or to the total protein content in the gel [33] determined with the help of stain-free technology (Bio-Rad) according to the manufacturer's instructions.

Light microscopy. Placentas were fixed in 10% neutral formalin solution for 24 h. Tissue dehydration was carried out with a vacuum infiltration processor Histo-Tek VP1 (Sakura, Japan); paraffin blocks were formed with a TES99 paraffin embedding center (Medite, Germany). Tissue sections (3-4 μm thick) were prepared with a Rotary 3002 microtome (PFM, Germany) and stained with hematoxylin-eosin. Light microscopy was used for examination of the placental labyrinth, basal zone (spongiotrophoblast), layer of trophoblast giant cells (TGCs), and blood cells. Microphotographs were acquired at 200× and 400× magnification with a system consisting of a light microscope Olympus CX43 (Olympus, Japan), color digital camera VideoZavr Standart VZ-18C23-B, and the VideoZavr Catalog database (ATM-praktika, Russia). Images with tissue defects, staining defects, and artefacts were eliminated from analysis. Quantitative morphometric analysis was carried out with the VideoTest-Morphology 5.2 program (Videotest, Russia). The trophoblastic septa (tissue between the maternal sinusoids and fetal capillaries) cross-sectional area in the placental labyrinth, as well as TGCs nuclei cross-sectional area were determined in each section in 5-7 fields of view, and the relative area of the investigated component (ratio of the component area to the total sample area) was calculated according to equation (1):

$$S\ (\%) = (S\ \text{component}/S\ \text{total}) \times 100. \quad (1)$$

Analysis of the cross-sectional area of erythrocyte aggregates in the labirynth zone was carried out in the areas of 1 mm^2 in 3-4 fields of view. Individual blood cells were not included in analysis; maternal and fetal blood spaces were not differentiated.

The thickness of the basal zone and placental labirynth was evaluted in the whole placenta cross-sections performed at the level of umbicial cord attachment. The ratio of the basal zone thickness to the labirynth zone thickness was determined.

Electron microscopy. Placenta tissues were washed with physiological saline to remove blood, immersed into a fixing solution (0.1 M PBS, pH 7.4, containing 1% glutaraldehyde and 1% formaldehyde) for 2 h, and then additionally fixed in 1% OsO_4 for 1 h. Tissue samples were contrasted with uranyl acetate, dehydrated, and embedded into an epon resin according to the protocol described in our previous studies [34, 35]. Ultrathin sections (thickness, 50 nm) were prepared with a Leica ultramicrotome (Leica Microsystems, Germany) and examined with a transmission electron microscope FEI Tecnai Spirit V2 (FEI, USA). Two placentas (each from different animal) from each group (control and experimental) were analyzed.

Placental barrier permeability was evaluated using a technique based on fluorometric detection of the amount of Evans Blue dye penetrated into the fetal tissues [36, 37]. Pregnant rats in the control and experimental groups were injected under Zoletil anesthesia (Zoletil 100; Virbac, France; 30 mg/kg of body weight) with solution of Evans Blue (45 mg in 0.5 ml of water) through the tail vein catheter on GD20 (3 h prior to decapitation). The animals were decapitated, the fetuses were taken out, and their brains and abdominal cavity organs (intestine, stomach, pancreas, etc., with exception of liver) were isolated for further investigation. Samples of isolated organ were immersed into formamide (6 ml per 1 g of organ weight), homogenized in this solution, and incubated for 18 h at 60°C to extract Evans Blue. The homogenates were centrifuged for 30 min in at 10,000 rpm using a Microspin12 centrifuge (BioSan, Latvia), and the supernatants containing formamide with extracted Evans Blue were collected. Fluorescence intensity of each sample was measured in two replicates with a CLARIOstar plus plate reader (BMG Labtech, Germany) at the excitation wavelength of 620 nm and emission wavelength of 670 nm. The average fluorescence value for each sample was corrected for the control sample (pure formamide) fluorescence. To eliminate the possibility of erroneous measuring tissue autofluorescence, the homogenates of the corresponding fetal tissue from animals injected with 0.5 ml of physiological saline without Evans Blue were used as a negative control.

Statistical data processing. The differences between the groups were evaluated with the STATISTICA 10.0 and GraphPad Prism 8 programs. The outliers were identified using the Grubbs test. The data were examined for the normality of distribution using the Shapiro–Wilk test; the homogeneity of dispersions was analyzed with the Levene's test. Depending on the type of parameter distribution in the datasets, control and experimental groups were compared using the Student's *t*-test (normal distribution, homogeneous dispersions), Welch's *t*-test (normal distribution, non-homogeneous dispersions), or non-parametric Mann–Whitney *U*-test (non-normal distribution). Significance threshold *p*-value was set at 0.05.

The study results in the figures and tables are presented either as mean ± standard error of mean (SEM) or median and quartiles (Me (Q_1; Q_3)).

RESULTS

Effect of methionine-induced HHcy on the body weight of pregnant rats and weight of their placentas and fetuses. The methionine load did not cause any significant changes in the weight gain of pregnant rats. The slopes of the curves describing the dependence of body mass on the gestational period were 5.20 ± 1.17 and 5.30 ± 1.24 in the control and experimental group, respectively. At the same time, maternal HHcy caused a significant reduction in the weight of fetuses and placentas on GD20 (Table 1).

Changes in the content of free AAs in the blood of female rats and their fetuses in methionine-induced maternal HHcy. Pregnant rats with the methionine-induced HHcy demonstrated an increase in the serum level of the majority of essential (His, Ile, Val, Lys, Phe, Trp) and non-essential (Ala + Arg, Asp, Gln, Tyr, Pro) AAs on GD20, which was also manifested as an increase in the total AA content (Table 2). On the contrary, the concentration of Asn in the maternal blood under the HHcy conditions is decreased. Fetal serum levels of some essential (Met, Trp) and non-essential (Gln, Ser) AAs were reduced in the case

Table 1. Effect of maternal HHcy on the fetal and placental weight on GD20

Fetal weight (mg)		Placental weight (mg)	
Control	HHcy	Control	HHcy
4182.2 ± ± 79.7	3491.3 ± ± 101.9***	570.1 ± ± 17.4	472.1 ± ± 8.1***

Note. The data are presented as mean ± SEM for the average mass of all fetuses or placentas in a litter from each dam; n = 13, dams in the control group, n = 16, dams in the group with HHcy; *** $p < 0.001$, Student's t-test.

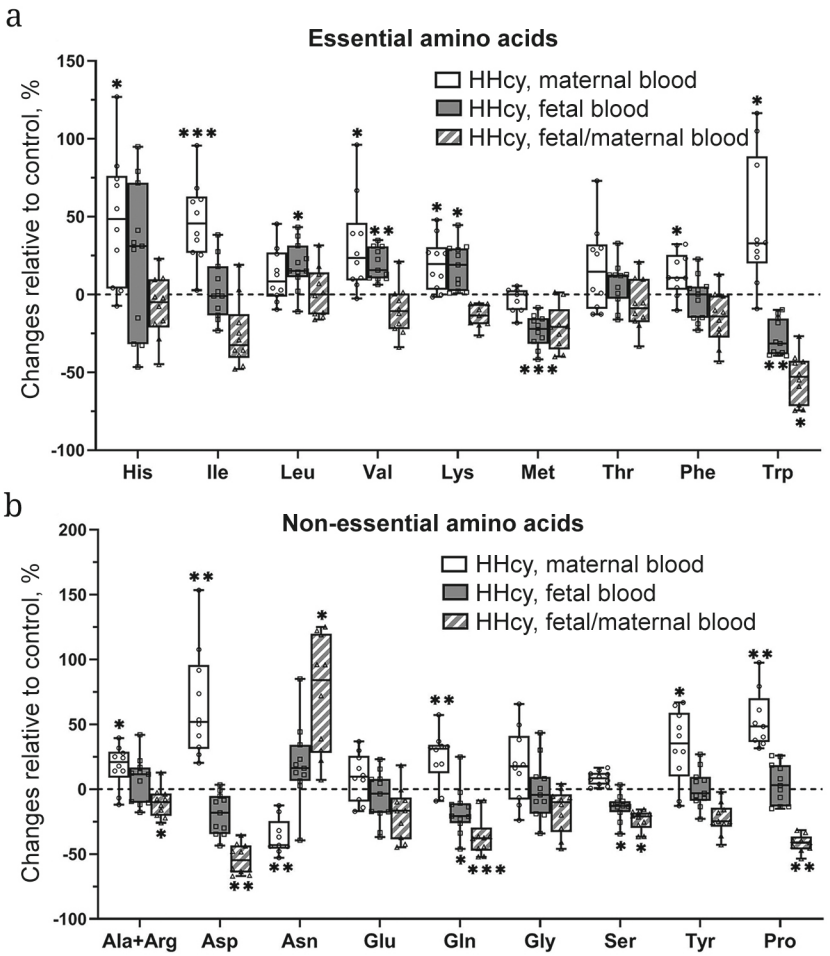

Fig. 1. Effect of maternal HHcy on the free AAs serum levels in pregnant rats and their fetuses, and on the ratio of fetal to maternal AAs serum content on GD20. Changes are shown as percent relatively to the control group; the data are presented as Me (Q_1; Q_3); n = 11, dams in the control group; n = 10, dams in the HHcy group; * $p < 0.05$, ** $p < 0.01$, *** $p < 0.001$ in comparison with the control; t-test or Mann–Whitney U-test.

Table 2. Serum concentrations of free amino acids (μmol/liter) in pregnant rats and their fetuses on GD20 under normal conditions and in the case of methionine-induced maternal HHcy

	AA	Maternal blood		Fetal blood	
		Control	HHcy	Control	HHcy
Essential AAs	His	27.4 ± 3.0	40.4 ± 3.7*	69.0 ± 12.2	84.9 ± 10.1
	Ile	90.1 ± 4.5	132.1 ± 7.5***	255.5 ± 15.2	262.9 ± 15.2
	Leu	107.3 ± 8.6	120.3 ± 5.8	249.3 ± 14.9	295.1 ± 11.6*
	Val	117.1 ± 9.6	153.5 ± 11.3*	373.7 ± 19.5	445.8 ± 11.6**
	Lys	462.1 ± 28.4	552.2 ± 24.8*	867.2 ± 45.1	1023.4 ± 38.5*
	Met	44.4 ± 1.6	42.9 ± 1.2	133.9 ± 5.8	102.4 ± 4.5***
	Thr	530.5 ± 28.2	619.0 ± 46.3	1063.4 ± 51.7	1133.1 ± 45.1
	Phe	58.0 ± 2.8	65.6 ± 2.5*	247.6 ± 11.3	241.5 ± 10.6
	Trp	51.1 ± 6.7	74.4 ± 6.7*	143.1 ± 9.9	102.9 ± 5.1**
	Branched-chain AAs (Ile + Leu + Val)	301.2 ± 17.7	405.9 ± 23.1*	878.4 ± 43.7	1003.7 ± 31.7*
	Total essential AAs	1434.0 ± 69.7	1800.4 ± 98.8*	3402.5 ± 86.2	3682.9 ± 105.1*
Non-essential AAs	Ala + Arg	845.0 ± 28.4	993.6 ± 43.3*	1464.0 ± 55.6	1562.2 ± 78.7
	Asp	22.2 ± 2.8	36.7 ± 3.0 **	68.6 ± 5.6	55.4 ± 3.3
	Asn	79.5 ± 2.7	50.3 ± 3.6 **	103.2 ± 6.3	123.3 ± 9.4
	Glu	120.7 ± 9.8	131.9 ± 7.0	362.4 ± 25.8	339.8 ± 21.6
	Gln	859.3 ± 31.9	1069.5 ± 54.6**	1655.9 ± 79.1	1377.3 ± 90.9*
	Gly	170.9 ± 11.3	201.2 ± 15.1	356.5 ± 24.2	355.1 ± 24.2
	Ser	290.1 ± 12.4	314.5 ± 4.8	441.3 ± 18.4	380.8 ± 13.2*
	Tyr	30.2 ± 2.0	40.1 ± 2.7 *	171.7 ± 18.7	172.9 ± 7.6
	Pro	206.4 ± 9.9	317.0 ± 15.3***	536.4 ± 18.9	559.7 ± 25.0
	Total non-essential AAs	2624.2 ± 68.3	3154 ± 86.5**	5160.0 ± 163.1	4926.5 ± 205.6
Total AA concentration		4109.7 ± 127.5	4955.1 ± 115.5***	8562.5 ± 203.8	8618.2 ± 245.3

Note. The data are presented as mean ± SEM; n = 11, dams in the control group; n = 10, dams in the HHcy group; * $p < 0.05$, ** $p < 0.01$, *** $p < 0.001$ in comparison with the control; t-test or Mann–Whitney U-test.

of maternal HHcy, while the content of essential AAs Val and Lys was increased. The total content of essential AAs in the serum of these fetuses was higher than in the control; at the same time, the total amount of non-essential AAs, as well as the total amount of all AAs did not change significantly. In the case of maternal HHcy, the ratio between the fetal and maternal concentrations of AAs was decreased (Ile, Met, Trp, Asp, Gln, Pro) or not changed (Asn was an exception, as the ratio for this AA was increased) (Fig. 1).

Effect of methionine-induced maternal HHcy on the neutral AA transporters content in the labirynth zone of rat placenta. In the case of methionine-induced HHcy, we observed an increase in the content of the sodium-dependent neutral AA transporter 2 (SNAT2; $p < 0.01$) and the L-type AA transporter 1

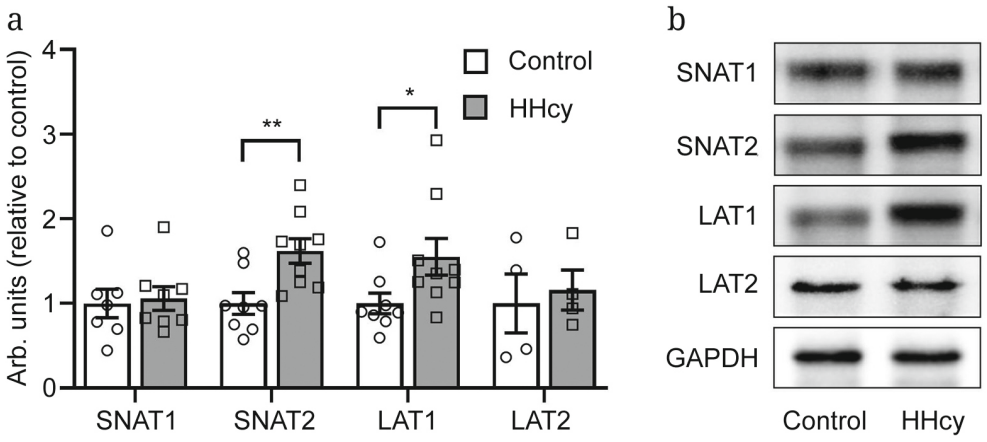

Fig. 2. Effect of maternal HHcy on the neutral AA transporters content in the labyrinth zone of rat placenta on GD20. The content of SNAT1, SNAT2, LAT1, and LAT2 proteins in the FPP in the control and HHcy groups (a), and representative immunoblot (b); *y*-axis, intensity of protein bands in immunoblots, arbitrary units; the data are shown as mean ± SEM; n = 4-8 dams in each group; * $p < 0.05$, Mann–Whitney *U*-test; ** $p < 0.01$, Student's *t*-test.

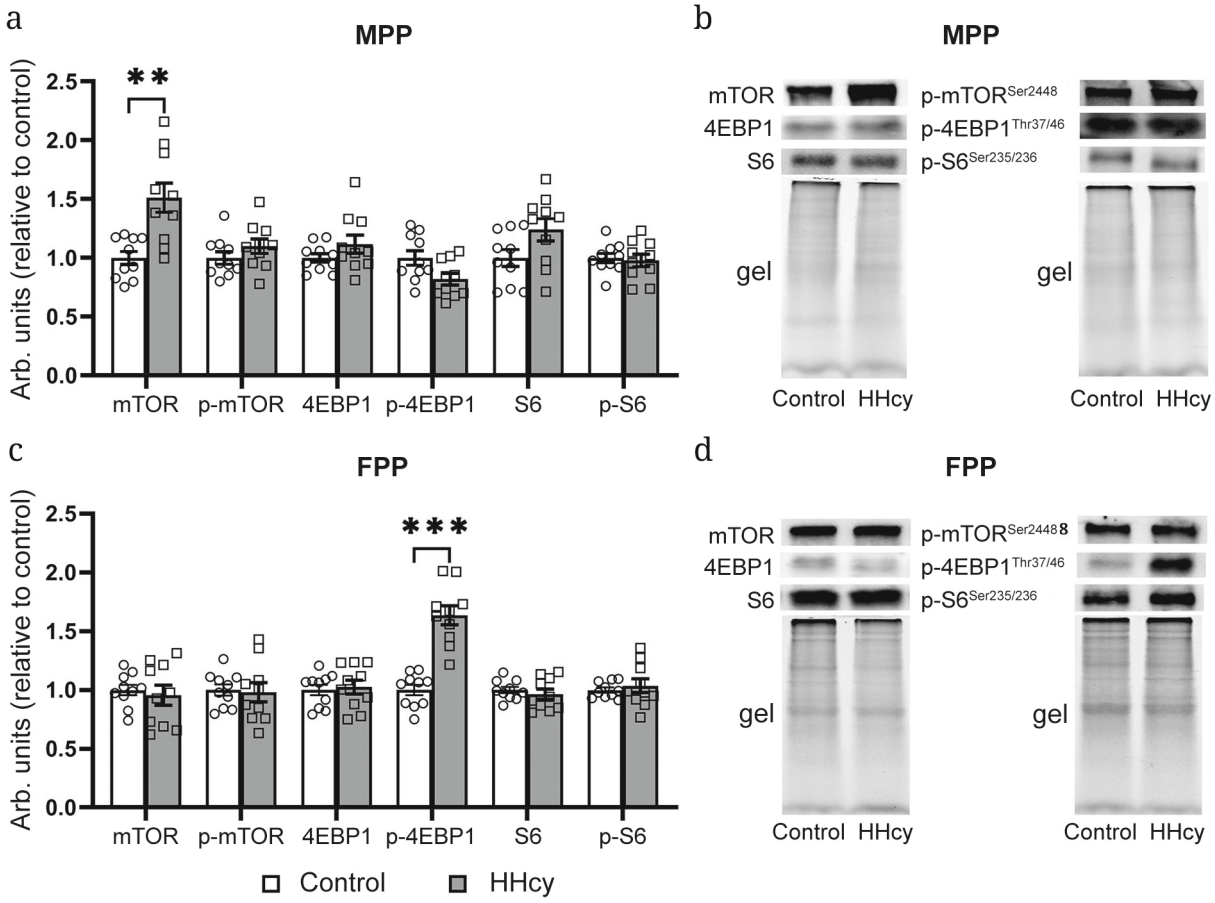

Fig. 3. Effect of maternal HHcy on mTORC1 signaling in different parts of rat placenta on GD20. The content of mTOR, 4E-BP1, and S6 proteins and their phosphorylated forms p-mTOR^{Ser2448}, p-4E-BP1$^{Thr37/46}$, and p-S6$^{Ser235/236}$ in the control and HHcy groups in the MPP (a) and FPP (c), and representative immunoblots/gels for MPP (b) and FPP (d); *y*-axis, intensity of protein bands in immunoblots, arbitrary units; the data are shown as mean ± SEM; n = 10 dams in each group; ** $p < 0.05$, Welch's *t*-test; **** $p < 0.001$, Student's *t*-test.

of large neutral AAs (LAT1; $p < 0.05$) in the FPP (labirynth zone) in pregnant rats on GD20 in comparison with the control animals (Fig. 2, a and b). At the same time, the level of the SNAT1 and LAT2 transporters in the FPP in the experimental and control animals did not differ significantly (Fig. 2, a and b).

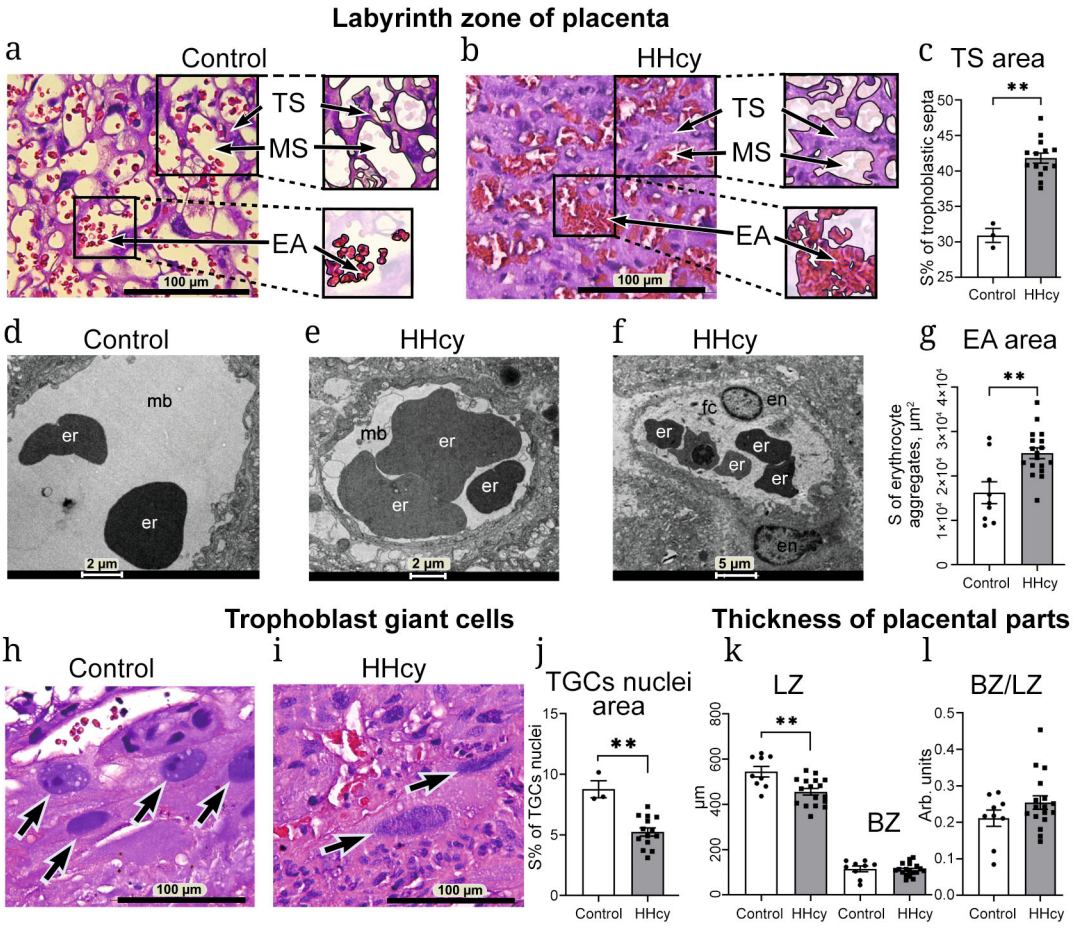

Fig. 4. Morphological changes in the placenta in rats with maternal HHcy on GD20. a, b) Labyrinth zone of placenta with trophoblastic septa (TS) and maternal sinusoids (MS) in the control (a) and HHcy (b) animals. Insets show the components which relative areas were calculated: TS and erythrocyte aggregates (EA); hematoxylin-eosin staining; magnification, ×200. c) Relative area (S%) of TS in the control and HHcy group. d-f) TEM images of placenta in the control (d) and HHcy (e and f) animals; mb, maternal blood in maternal sinusoid; fc, fetal capillary; er, erythrocytes in maternal sinusoids (d and e) and fetal capillary (f); en, fetal capillary endothelium. g) Area of EA in the labyrinth zone of placenta in the control and HHcy group. h, i) Trophoblast giant cells (TGCs) in the control (h) and HHcy (i) animals; hematoxylin-eosin staining; magnification, ×400; TGCs nuclei are shown with arrows. j) Relative area (S%) of TGCs nuclei in the control and HHcy group. k) Thickness of the labyrinth zone (LZ) and basal zone (BZ) of the placenta. l) BZ thickness to LZ thickness ratio. All data are presented as mean ± SEM. In panels (c) and (j), $n = 3$ placentas from 3 dams in the control group, $n = 14$ placentas from 4 dams in the HHcy group; in panels (g), (k), and (l), $n = 9$ placentas from 5 dams in the control group, $n = 18$ placentas from 6 dams in the HHcy group; ** $p < 0.01$, Student's *t*-test.

Effect of methionine-induced maternal HHcy on the activity of mTORC1 signaling in different regions of rat placenta. The content of mTOR protein was increased ($p < 0.05$) in the MPP (contains mainly the bazal zone of placenta) in rats with the experimental HHcy on GD20; however, no changes in the phosphorylated mTOR or downstream components of the mTORC1 signaling cascade were observed (Fig. 3, a and b). HHcy did not affect the extent of mTOR phosphorylation or the content and phosphorylation level of the ribosomal protein S6 (downstream effector of the mTORC1 complex) in the FPP (labirynth zone); however, we observed activation of eukaryotic translation initiation factor 4E-binding protein 1 (4E-BP1), another downstream target of mTORC1, which was manifested as an increase in its phosphorylation at Thr37/46 ($p < 0.001$; Fig. 3, c and d).

Structural changes in placental tissues in maternal HHcy. The placental labyrinth (corresponding to FPP) is an exchange zone between the maternal and fetal circulations. In control on GD20 it composed of a branched network of thin intersecting trophoblastic septa which contain the trophoblast cells and fetal blood capillaries, and the wide maternal sinusoids filled with maternal blood (Fig. 4, a and b). In animals with HHcy, the trophoblastic septa in the labyrinth zone were thickened in comparison with the control ($p < 0.01$; Fig. 4, b and c); correspondingly, the relative area of the sinusoids was decreased. Narrowing of maternal sinusoids was accompanied by the blood stasis

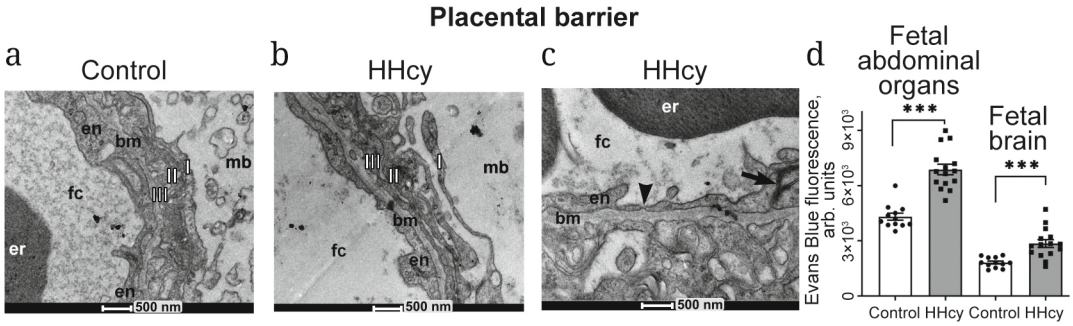

Fig. 5. Effect of maternal HHcy on the ultrastructure and permeability of rat placental barrier on GD20. a-c) TEM images of the exchange zone between the maternal and fetal circulatory systems in the placental labyrinth; mb, maternal blood in maternal sinusoid; fc, fetal capillary; placental barrier layers: I, cytotrophoblast layer in contact with maternal blood, II and III, two STB layers; bm, basal membrane lining the fetal capillary endothelium (en); er, erythrocyte in the vessel lumen; arrow, tight contact between endothelial cells; arrowhead, fenestra in the fetal capillary endothelium. d) Fluorescence of Evans Blue dye in the tissues of fetal abdominal organs and brain 3 h after dye injection to rat females; n = 12 placentas from 2 dams in the control group, n = 15 placentas from 2 dams in the HHcy group; *** $p < 0.001$, Welch's t-test.

and erythrocyte aggregation (Fig. 4, a and b). Accumulation of erythrocytes in the lumen of the smallest maternal sinusoids and fetal cappilaries has been also observed during examination of the labyrinth zone ultrastructure (Fig. 4, d-f). The increase in the erythrocyte aggregates area in the labyrinth zone was also confirmed by the morphometric data ($p < 0.01$; Fig. 4g).

The basal zone of the placenta contains three types of cells: spongiotrophoblasts, glycogen cells, and trophoblast giant cells (TGCs) forming a thin layer at the border between the basal zone and decidua basalis and performing the endocrine function. In the control group, TGCs formed a layer with a thickness of 2-3 cells with the oxyphilic cytoplasm, roundish-oval nuclei, and uniform chromatin distribution (Fig. 4h). In the group with maternal HHcy, the TGCs layer was thinner and consisted of 1-2 cells that demonstrated vacuolar degeneration (Fig. 4i). In some samples from the experimental animals, TGCs lacked the nuclei; some individual cells displayed karyolysis. The relative area of TGCs nuclei decreased in HHcy ($p < 0.01$; Fig. 4j).

Animals with maternal HHcy on GD20 demonstrated reduction in the thickness of the labyrinth zone ($p < 0.05$; Fig. 4k), while the thickness of the basal zone, as well as the ratio of the basal zone thickness to the thickness of the labyrinth zone did not change significantly (Fig. 4, k and l).

Effect of maternal HHcy on the permeability of placental barrier. The ultrastructural studies of the exchange zone between the maternal and fetal circulation in the placental labyrinth showed that in some rats with HHcy, there was a disintegration of the three layers comprising the placental barrier (I, cytotrophoblast layer in contact with maternal blood; II, first STB layer, and III, second STB layer in contact with the basement membrane of fetal capillary endothelium), which resulted in the formation of gaps between their membranes (Fig. 5, a and b). The number of fenestrae closed by the diaphragms in the fetal vessels endothelium is increased (Fig. 5c). Penetration of Evans blue dye through the placental barrier was significantly higher in animals with HHcy, which was manifested as an increasing of the dye fluorescence in the fetal abdominal organs and brain in the experimental group in comparison with the control ($p < 0.001$; Fig. 5d).

DISCUSSION

Currently, administration of methionine, either with food and drinking water or via an oral gavage, is the most popular method for modeling HHcy in animals [38, 39]. In comparison with direct administration of Hcy, it ensures higher intracellular levels of Hcy typical for clinical HHcy cases in humans [40]. However, an unavoidable feature of this model is that, in addition to the increasing of the Hcy blood level, it leads to simultaneous elevation of the methionine blood content, which can affect the balance of free AAs in blood [41]. In our previous study, we examined the dynamics of Hcy content in the blood of female rats and their fetuses in our HHcy model that involved daily administration of methionine through a gastric tube to rat females [29]. The concentration of Hcy in the blood of pregnant rats on GD20 (5.7 ± 0.2 μmol/liter before the treatment) increased to 87.2 ± 24.2 μmol/liter already 1 h after oral administration of methionine and was maintained at an approximately same high level (81.4 ± 31.3 μmol/liter) for 6 h after its administration. This was followed by a gradual decrease in the Hcy content, which, however, remained significantly higher (34.1 ± 14.7 μmol/liter) than in the control up to 18 h after methionine loading and reached the level close to the normal one (6.6 ± 0.5 μmol/liter) only after 24 h, right before the next methionine administration [29]. Similar changes in the Hcy concentration were observed

in the fetal blood after methionine administration to mothers [29]. An increase in the Hcy level in the blood after methionine administration should be preceded by methionine transport into cells, its metabolic transformation into Hcy, and export of the formed Hcy back into the blood. Due to this, the level of methionine itself reaches its peak in the blood and returns to the normal values prior to the corresponding changes in the Hcy content [42]. Hence, the absence of increase in the methionine concentration in the blood of rat females and their fetuses 24 h after methionine administration in our study is quite natural. We hypothesize that in our model, the effects of the increased Hcy content, as a more long-term acting factor in comparison with the short-term increase in the methionine level, overcome the effects of methionine.

Consumption of AAs with food at the doses significantly exceeding the requirements for these compounds causes toxic effects in animals [43]. Moreover, the adverse effect of the methionine excess in the diet is more pronounced in comparison with the excess of other AAs and is manifested primarily as a decrease in food intake and organism growth suppression [43]. The fetuses of pregnant animals receiving food with the excess of methionine also demonstrated growth restriction [13, 44]. In our study, the weight gain in female rats exposed to methionine was the same as in the control animals, which indicated the absence of significant differences in the food consumption between the groups. The toxic effect of methionine-induced HHcy was manifested as a reduction in fetal weight, which was in agreement with the results of our earlier studies [29, 30].

We found that chronic administration of methionine increased the content of the majority of essential (His, Ile, Val, Lys, Phe, Trp) and non-essential (Ala + Arg, Asp, Asn, Gln, Tyr, Pro) AAs in the blood of female rats on GD20, which was also reflected as an increase in the total level of essential and non-essential AAs. Indeed, it has been reported before that the blood content of AAs was increased in animals with HHcy caused by genetic defects in enzymes involved in Hcy metabolism or in those consuming food enriched with methionine [12, 14-16]. Methionine-enriched diet containing only 1.6-fold excess of methionine caused an increase in the Hcy level in the mouse blood, while in order to increase the concentration of methionine and other AAs in the blood, the content of methionine in food had to be increased up to 7-10-fold [16]. This fact implies the existence of adaptive mechanisms aimed at eliminating an excess of methionine in the blood, primarily via its transformation into Hcy, which emphasizes the significance of Hcy as a key toxic agent in the case of methionine loading.

It is possible that the increase of the level of free AAs during methionine loading is mediated by some metabolic mechanisms. For example, methionine catabolism through Hcy involves enzymes (propionyl-CoA carboxylase) and intermediate products (propi-branched-chain AAs catabolic pathways [45]. An excess of one or several intermediates formed in the course of methionine metabolism, could slow down the catabolism of other AAs sharing these pathways with methionine. However, in our study, we observed in the maternal blood increased levels not only of branched-chain AAs, but also of other essential and non-essential AAs, whose metabolism is not directly associated with the metabolism of methionine and Hcy. It has been assumed that the excess of methionine and Hcy in the blood could reduce the transport of other AAs by competing with them for common AA transporters [16, 17, 46]. Our data supports the hypothesis that methionine-induced HHcy can cause the downregulation of AA transport to the maternal cells and/or to the fetal circulation through the placenta resulting in AAs accumulation in the mother's blood.

The total level of all AAs in the fetal blood did not change in HHcy. Although the concentration of two essential AAs (Val and Lys) in the fetal blood from the HHcy group increased (similar to the maternal blood), the content of Met, Gln, Trp, and Ser in the fetal blood was significantly lower in comparison with the control. Moreover, the fetal/maternal blood content ratio of Pro and Ala + Arg levels in the experimental group was also decreased in comparison to the control. The AAs, which levels was reduced in the fetal blood under the HHcy condition, are the substrates of the placental transport systems L (Met, Gln, Trp, Ala, Ser), A (Met, Gln, Ala, Ser, Pro), and y^+L (Arg, Gln, Met) [17, 47]. It has been suggested that Hcy could be the substrate of transporters of the system A (SNAT1, SNAT2 and SNAT4), L (LAT1, LAT2), and y^+L (y^+LAT1, y^+LAT2) [17, 18], hence, the reduction in the aforementioned AAs content in the fetal blood is in agreement with the hypothesis on the competitive inhibition of their placental transport in maternal HHcy.

Gln and its precursor Glu are vital for fetal growth and development. The concentration of Gln in maternal and fetal blood, as well as the rate of its mother-to-fetus transport, are the highest among other AAs [48, 49]. The required levels of Gln and Glu in the fetal blood are maintained due to the ability of these AAs to interconvert and recirculate between the placenta and fetal liver [48]. The observed decrease in the Gln level in the fetal blood could be caused by its increased consumption to compensate for the fetal growth restriction in maternal HHcy.

Negatively charged AAs (Asp and Glu) are transported from mother to fetus by the excitatory amino acid transporters of the EAAT group that belong to the transport system X^{AG} [47]. With methionine loading, an increase in the Asp concentration in the mother's

blood was observed, which was accompanied by a decrease in the ratio of the Asp level in the fetal blood to its content in the mother's blood. Methionine and Hcy are not the substrates of the EAAT transporters; hence, changes in the Asp level cannot be caused by the competition with Met and/or Hcy for the common transporters. The increase in the Asp level with simultaneous decrease in the Asn content in the maternal blood in HHcy can be associated with the decrease in the Asn synthesis from Asp. Considering that the synthesis of Asn from Asp requires Gln as the nitrogen donor [50], the decrease in the Gln content in the fetal blood in HHcy and simultaneous decrease in Asp fetal/maternal blood content ratio accompanied by the increase of this ratio for Asn could be interconnected.

As a precursor of serotonin (5-HT), maternal Trp is very important for the development of the fetal nervous system. In rodents, placenta starts to synthesize 5-HT from maternal Trp on GD10, and up to GD15, placental 5-HT remains the main and, probably, only source of this neurotransmitter in fetal brain [51, 52]. The decrease in the Trp concentration in fetal blood observed in this study could result in the decrease of 5-HT synthesis in fetal brain, thus negatively affecting brain development. Considering that in the rodent placenta, 5-HT is synthesized predominantly by the TGCs [53], the observed reduction in the number of these cells could contribute to the decrease in 5-HT available for the fetus.

In addition to the possible competition of Hcy with other AAs for common transporters, HHcy-associated morphological changes in the placenta could be the reason for a decreased mother-to-fetus AA transport [54]. In this study, we observed a decrease in the placenta weight, thickness of the labyrinth zone, and relative area of maternal sinusoids accompanied by the slowing of circulation and increased erythrocyte aggregation, which is a risk factor for the development of microthrombosis [55]. The decrease in the area of sinusoids, where maternal blood comes in contact with the STB layer, as well as slowing down of placental circulation result in the reduction of nutrient transport through the transporters located on the STB membranes [10]. Defects and deficiencies in the vascular tree formation in the labyrinth zone, which mediates the nutrient transport from a mother to a fetus, often results in the fetal growth restriction [54]. Morphological changes detected in the labyrinth zone in our study could, in part, be the consequences of the previously reported imbalance between angiogenic and growth factors in the placenta in the case of maternal HHcy [30].

As has been mentioned above, the mother-to-fetus transport of neutral AAs through the placenta in rodents and humans is realized primarily through the system A and L transporters, whose activity and expression on the STB membranes are controlled by the mTOR signaling [7, 17, 56]. Low amounts of nutrients in mother's diet during pregnancy cause a decrease in the activity of the mTORC1 complex in the placenta and downregulation of AA transporters expression and activity on the STB membranes, which is accompanied by a reduction in the fetal weight [7]. On the other hand, an excess of nutrients in the maternal blood causes activation of the mTORC1 complex and upregulation of AA transporters expression in the placenta, resulting in the increase in the fetal weight [57, 58]. The effects of maternal HHcy, which is characterized by the excess of Hcy and, likely, some other AAs in the maternal blood, but simultaneously accompanied by the fetus growth restriction [1, 44], on activity of placental mTORC1 complex have not been investigated in detail.

Here, we attempted for the first time to evaluate the effects of maternal HHcy induced by chronic methionine loading, on activity of the mTORC1 complex in different morphological parts of the placenta using phosphorylation of the mTORC1 downstream effectors 4E-BP1 and S6 as functional markers. In the MPP, which is not directly associated with the transport of nutrients to the fetus, mTOR acts mostly as a stimulator of growth and functional maturation via activation of protein synthesis [59]. The observed increase in the total level of mTOR protein in the MPP in animals with HHcy could be a compensatory response to the reduction of the endocrine function of this placental region which requires continuously high level of protein synthesis [60]. In this study the number of TGCs cells, which are the main endocrine cells in the MPP [61], was found to decrease in maternal HHcy. The level of phosphorylated 4E-BP1 protein in the labyrinth zone was increased; at the same time, no changes in the expression of total mTOR protein or its phosphorylated at Ser2448 form, as well as no activation of S6 protein (another target of mTOR) were observed. At present, several mTOR phosphorylation sites have been identified, but their functional significance is still poorly understood [62]. It was shown that mTOR is phosphorylated at Ser2448 by the downstream kinase S6K1, which is also responsible for S6 protein phosphorylation [63]. Hence, the absence of changes in the levels of p-mTOR^{Ser2448} and p-S6 could be due to the unchanged activity of S6K1 kinase. Activation of 4E-BP1 could be caused by either activation of mTOR through phosphorylation at other sites or by the action of mTOR-independent kinases [64]. It should be mentioned that unidirectional and simultaneous changes in the levels of p-mTOR, p-4E-BP1, and p-S6 are not always detected in studies investigating effects of the mTOR signaling on the fetal growth [5].

The observed in HHcy increase in the LAT1 and SNAT2 neutral AA transporters content in the labyrinth

zone could be caused by the 4E-BP1 signaling pathway activation resulting in the increase in the corresponding proteins synthesis and transport to the STB membranes [11]. On the other hand, it has been suggested that the increase of the number of AA transporters in the placenta could be a compensatory response to the reduction of the mother-to-fetus AA transport [7]. A compensatory increase in the expression of the Gln transporter LAT1 has been observed in the placentas with a reduced mass and, subsequently, decreased surface area of exchange between the maternal and fetal blood [48]. However, this adaptation is not always capable to fully replenish an insufficient AA supply to the fetus, which results in the fetal growth restriction even in the presence of a higher number of AA transporters and increase in the relative transporting capacity of the placenta [48].

The exchange zone between the maternal and fetal blood in the rat placental labyrinth consists of three trophoblast layers: permeable cytotrophoblast layer in direct contact with the maternal blood in sinusoids and two continuous STB layers underneath it, which comprise the structural basis of the placental barrier [56]. The integrity of the placental barrier is crucial for normal fetal growth and development [65]. The observed increase in the penetration of Evans Blue dye, which is transported by albumin and other proteins in maternal blood [66], into abdominal organs and brain of the fetuses could result from the increased permeability of the placenta for macromolecules [67]. Earlier, we demonstrated an increase in the levels of the proangiogenic factor VEGF-A, a known inducer of placental permeability [65, 67], in the FPP on GD20 in rats with HHcy [30]. The morphological basis of the increased permeability of the placental barrier could be disintegration of its layers observed in some cases, as well as increase in the number of fenestrae in the fetal capillary endothelium. It was shown that some maternal proteins could be transferred across the placental barrier into the fetal circulation by endocytosis/exocytosis across the STB or via the paracellular diffusion through the STB nanopores [68, 69]. Proteins internalized by macropinocytosis could be catabolized in STB lysosomes and serve as additional sources of AAs for the placenta and the fetus [70]. Such metabolic pathway was shown for albumin internalization by the STB membrane in the human placenta; in the process, molecules transported by this protein are released to the intracellular STB compartments [71] and can possibly be transported further to the fetal circulation. Therefore, an increase in the penetration of Evans blue dye into fetal tissues could also be a consequence of an increase in the uptake of albumin and other dye-binding proteins by the STB to compensate for the requirements of the placenta and fetus for AAs in conditions of its reduced growth.

This study was based on the hypothesis that maternal HHcy can inhibit the placental transport of some AAs, which are shared with Hcy common transport mechanisms mediated by the placental neutral AA transport systems A and L. We did not investigate the effect of HHcy on the expression of the y^+L system transporters, which presumably can also transport Hcy [17]. The possible influence of sulfur-containing compounds formed in the course of Hcy metabolism on the placental transport of AAs was also left outside our consideration. The main metabolite formed in the process of the Hcy catabolism via transsulfuration is Cys. It has been noted that an increase in the total Hcy level in the blood could be accompanied with a decrease in the total content of Cys [16, 72]. In the blood, Cys is present mostly in its oxidized dimeric form (cystine), which is transported across the maternal-facing STB membrane with the help of xCT/SLC7A11 transporter of the Xc^- transport system [73]. In STB, cystine is reduced to Cys and serves as a precursor for the synthesis of glutathione (GSH), thus enhancing the antioxidant defense of the placenta [73]. Although GSH could be formed in the process of Hcy transsulfuration, the content of its reduced form and/or the ratio between its reduced and oxidized forms in the blood and brain are decreased in HHcy, which has been associated with GSH oxidation caused by the HHcy-induced oxidative stress [16, 74]. The decrease in the total content of Cys and GSH level in the maternal blood is accompanied with the decrease in the GSH level and promotion of the HHcy-induced oxidative stress in the placenta [30], which could contribute to the negative effect of maternal HHcy on the placental development and transport function.

The results obtained in this study indicate that maternal HHcy in rats causes poor vascular development in the labyrinth zone of placenta, decrease in the content of some AAs in the fetal blood, and increase in the permeability of the placental barrier. Reduced levels of some AAs in the fetal blood in HHcy can be consequence of inhibition of their placental transport due to competition with Hcy for common transporters, as well as decreasing in the surface area of exchange zone between maternal and fetal circulations due to narrow maternal sinusoids. The signaling from the fetal side about the decrease in the content of some AAs in the fetal blood and fetal weigh reduction might induce an adaptive response in the placenta manifested as the activation of 4E-BP, a downstream effector of the mTORC1 complex, and increase in the number of neutral AA transporters LAT1 and SNAT2 in the labyrinth zone of the placenta.

Acknowledgments. The authors are grateful to A. N. Kadenov, A. V. Gorbova, and V. A. Poda for their help in conducting experiments.

Contributions. A.V.A. supervised the study and edited the manuscript; Yu.P.M. and G.O.K. developed the study concept and wrote the text of the article; Yu.P.M., G.O.K., and D.S.V. discussed the study results; I.V.Z., S.K.B., A.V.M., G.Kh.T., N.L.T., and D.S.V. conducted the experiments and collected the data; Yu.P.M., A.D.Sh., and D.S.V. analyzed the data.

Funding. This study was supported by the Russian Science Foundation (project no. 22-15-00393).

Ethics declarations. All applicable international, national, and/or institutional guidelines for the care and use of animals were followed. The authors of this work declare that they have no conflicts of interest.

REFERENCES

1. Dai, C., Fei, Y., Li, J., Shi, Y., and Yang, X. (2021) A novel review of homocysteine and pregnancy complications, *Biomed. Res. Int.*, **2021**, 6652231, https://doi.org/10.1155/2021/6652231.
2. Gaiday, A., Balash, L., and Tussupkaliyev, A. (2022) The role of high concentrations of homocysteine for the development of fetal growth restriction, *Rev. Bras. Ginecol. Obstet.*, **44**, 352-359, https://doi.org/10.1055/s-0042-1743093.
3. Memon, S. I., Acharya, N. S., Acharya, S., Potdar, J., Karnik, M., and Mohammad, S. (2023) Maternal hyperhomocysteinemia as a predictor of placenta-mediated pregnancy complications: a two-year novel study, *Cureus*, **15**, e37461, https://doi.org/10.7759/cureus.37461.
4. Gaccioli, F., Lager, S., Powell, T. L., and Jansson, T. (2013) Placental transport in response to altered maternal nutrition, *J. Dev. Orig. Health Dis.*, **4**, 101-115, https://doi.org/10.1017/S2040174412000529.
5. Dong, J., Shin, N., Chen, S., Lei, J., Burd, I., and Wang, X. (2020) Is there a definite relationship between placental mTOR signaling and fetal growth? *Biol. Reprod.*, **103**, 471-486, https://doi.org/10.1093/biolre/ioaa070.
6. Jansson, T., Aye, I. L., and Goberdhan, D. C. (2012) The emerging role of mTORC1 signaling in placental nutrient-sensing, *Placenta*, **33**, e23-e29, https://doi.org/10.1016/j.placenta.2012.05.010.
7. Chassen, S., and Jansson, T. (2020) Complex, coordinated and highly regulated changes in placental signaling and nutrient transport capacity in IUGR, *Biochim. Biophys. Acta Mol. Basis Dis.*, **1866**, 165373, https://doi.org/10.1016/j.bbadis.2018.12.024.
8. Kramer, A. C., Jansson, T., Bale, T. L., and Powell, T. L. (2023) Maternal-fetal cross-talk via the placenta: influence on offspring development and metabolism, *Development*, **150**, dev202088, https://doi.org/10.1242/dev.202088.
9. Sibley, C. P., Brownbill, P., Dilworth, M., and Glazier, J. D. (2010) Review: adaptation in placental nutrient supply to meet fetal growth demand: implications for programming, *Placenta*, **31**, S70-S74, https://doi.org/10.1016/j.placenta.2009.12.020.
10. Lewis, R. M., Brooks, S., Crocker, I. P., Glazier, J., Hanson, M. A., Johnstone, E. D., Panitchob, N., Please, C. P., Sibley, C. P., Widdows, K. L., and Sengers, B. G. (2013) Review: modelling placental amino acid transfer – from transporters to placental function, *Placenta*, **34**, S46-S51, https://doi.org/10.1016/j.placenta.2012.10.010.
11. Rosario, F. J., Dimasuay, K. G., Kanai, Y., Powell, T. L., and Jansson, T. (2016) Regulation of amino acid transporter trafficking by mTORC1 in primary human trophoblast cells is mediated by the ubiquitin ligase Nedd4-2, *Clin. Sci. (Lond)*, **130**, 499-512, https://doi.org/10.1042/CS20150554.
12. Matsueda, S., and Niiyama, Y. (1982) The effects of excess amino acids on maintenance of pregnancy and fetal growth in rats, *J. Nutr. Sci. Vitaminol. (Tokyo)*, **28**, 557-573, https://doi.org/10.3177/jnsv.28.557.
13. Mori, M., Yamashita, Y., Hiroi, Y., Shinjo, S., Asato, R., Hirai, K., Suzuki, K., and Yamamoto, S. (1999) Effect of single essential amino acid excess during pregnancy on dietary nitrogen utilization and fetal growth in rats, *Asia Pac. J. Clin. Nutr.*, **8**, 251-257, https://doi.org/10.1046/j.1440-6047.1999.00094.x.
14. Akahoshi, N., Kamata, S., Kubota, M., Hishiki, T., Nagahata, Y., Matsuura, T., Yamazaki, C., Yoshida, Y., Yamada, H., Ishizaki, Y., Suematsu, M., Kasahara, T., and Ishii, I. (2014) Neutral aminoaciduria in cystathionine beta-synthase-deficient mice; an animal model of homocystinuria, *Am. J. Physiol. Renal. Physiol.*, **306**, F1462-F1476, https://doi.org/10.1152/ajprenal.00623.2013.
15. Akahoshi, N., Yokoyama, A., Nagata, T., Miura, A., Kamata, S., and Ishii, I. (2019) Abnormal amino acid profiles of blood and cerebrospinal fluid from cystathionine beta-synthase-deficient mice, an animal model of homocystinuria, *Biol. Pharm. Bull.*, **42**, 1054-1057, https://doi.org/10.1248/bpb.b19-00127.
16. Ishii, I., Kamata, S., Ito, S., Shimonaga, A., Koizumi, M., Tsushima, M., Miura, A., Nagata, T., Tosaka, Y., Ohtani, H., Kamichatani, W., and Akahoshi, N. (2022) A high-methionine diet for one-week induces a high accumulation of methionine in the cerebrospinal fluid and confers bipolar disorder-like behavior in mice, *Int. J. Mol. Sci.*, **23**, 928, https://doi.org/10.3390/ijms23020928.
17. Tsitsiou, E., Sibley, C. P., D'Souza, S. W., Catanescu, O., Jacobsen, D. W., and Glazier, J. D. (2011) Homocysteine is transported by the microvillous plasma membrane of human placenta, *J. Inherit. Metab. Dis.*, **34**, 57-65, https://doi.org/10.1007/s10545-010-9141-3.
18. Tsitsiou, E., Sibley, C. P., D'Souza, S. W., Catanescu, O., Jacobsen, D. W., and Glazier, J. D. (2009) Homocysteine transport by systems L, A and y+L across the microvillous plasma membrane of human placenta,

J. Physiol., **587**, 4001-4013, https://doi.org/10.1113/jphysiol.2009.173393.
19. Tripathi, M., Zhang, C. W., Singh, B. K., Sinha, R. A., Moe, K. T., DeSilva, D. A., and Yen, P. M. (2016) Hyperhomocysteinemia causes ER stress and impaired autophagy that is reversed by Vitamin B supplementation, *Cell Death Dis.*, **7**, e2513, https://doi.org/10.1038/cddis.2016.374.
20. Witucki, L., and Jakubowski, H. (2023) Homocysteine metabolites inhibit autophagy, elevate amyloid beta, and induce neuropathy by impairing Phf8/H4K20me1-dependent epigenetic regulation of mTOR in cystathionine beta-synthase-deficient mice, *J. Inherit. Metab. Dis.*, **46**, 1114-1130, https://doi.org/10.1002/jimd.12661.
21. Khayati, K., Antikainen, H., Bonder, E. M., Weber, G. F., Kruger, W. D., Jakubowski, H., and Dobrowolski, R. (2017) The amino acid metabolite homocysteine activates mTORC1 to inhibit autophagy and form abnormal proteins in human neurons and mice, *FASEB J.*, **31**, 598-609, https://doi.org/10.1096/fj.201600915R.
22. Wang, M., Liang, X., Cheng, M., Yang, L., Liu, H., Wang, X., Sai, N., and Zhang, X. (2019) Homocysteine enhances neural stem cell autophagy in *in vivo* and *in vitro* model of ischemic stroke, *Cell Death Dis.*, **10**, 561, https://doi.org/10.1038/s41419-019-1798-4.
23. Zhao, Y., Huang, G., Chen, S., Gou, Y., Dong, Z., and Zhang, X. (2016) Homocysteine aggravates cortical neural cell injury through neuronal autophagy overactivation following rat cerebral ischemia-reperfusion, *Int. J. Mol. Sci.*, **17**, 1196, https://doi.org/10.3390/ijms17081196.
24. Kitada, M., Xu, J., Ogura, Y., Monno, I., and Koya, D. (2020) Mechanism of activation of mechanistic target of rapamycin complex 1 by methionine, *Front. Cell Dev. Biol.*, **8**, 715, https://doi.org/10.3389/fcell.2020.00715.
25. Ouyang, Y., Wu, Q., Li, J., Sun, S., and Sun, S. (2020) S-adenosylmethionine: a metabolite critical to the regulation of autophagy, *Cell Prolif.*, **53**, e12891, https://doi.org/10.1111/cpr.12891.
26. Rosario, F. J., Powell, T. L., and Jansson, T. (2017) mTOR folate sensing links folate availability to trophoblast cell function, *J. Physiol.*, **595**, 4189-4206, https://doi.org/10.1113/JP272424.
27. Chen, Q., Dai, W., Sun, Y., Zhao, F., Liu, J., and Liu, H. (2018) Methionine partially replaced by methionyl-methionine dipeptide improves reproductive performance over methionine alone in methionine-deficient mice, *Nutrients*, **10**, 1190, https://doi.org/10.3390/nu10091190.
28. Batistel, F., Alharthi, A. S., Wang, L., Parys, C., Pan, Y. X., Cardoso, F. C., and Loor, J. J. (2017) Placentome nutrient transporters and mammalian target of rapamycin signaling proteins are altered by the methionine supply during late gestation in dairy cows and are associated with newborn birth weight, *J. Nutr.*, **147**, 1640-1647, https://doi.org/10.3945/jn.117.251876.
29. Arutjunyan, A. V., Milyutina, Y. P., Shcherbitskaia, A. D., Kerkeshko, G. O., Zalozniaia, I. V., and Mikhel, A. V. (2020) Neurotrophins of the fetal brain and placenta in prenatal hyperhomocysteinemia, *Biochemistry (Moscow)*, **85**, 248-259, https://doi.org/10.1134/S000629792002008X.
30. Arutjunyan, A. V., Kerkeshko, G. O., Milyutina, Y. P., Shcherbitskaia, A. D., Zalozniaia, I. V., Mikhel, A. V., Inozemtseva, D. B., Vasilev, D. S., Kovalenko, A. A., and Kogan, I. Y. (2023) Imbalance of angiogenic and growth factors in placenta in maternal hyperhomocysteinemia, *Biochemistry (Moscow)*, **88**, 262-279, https://doi.org/10.1134/S0006297923020098.
31. Askretkox, A. D., Klishin, A. A., Zybin, D. I., Orlova, N. V., Kholodova, A. V., Lobanova, N. V., and Seregin, Yu. A. (2020) Determination of twenty proteinogenic amino acids and additives in cultural liquid by high-performance liquid chromatography, *J. Anal. Chem.*, **75**, 1038-1045, https://doi.org/10.1134/S1061934820080031.
32. Bradford, M. M. (1976) A rapid and sensitive method for the quantitation of microgram quantities of protein utilizing the principle of protein-dye binding, *Anal. Biochem.*, **72**, 248-254, https://doi.org/10.1006/abio.1976.9999.
33. Bass, J. J., Wilkinson, D. J., Rankin, D., Phillips, B. E., Szewczyk, N. J., Smith, K., and Atherton, P. J. (2017) An overview of technical considerations for Western blotting applications to physiological research, *Scand. J. Med. Sci. Sports*, **27**, 4-25, https://doi.org/10.1111/sms.12702.
34. Shcherbitskaia, A. D., Vasilev, D. S., Milyutina, Y. P., Tumanova, N. L., Mikhel, A. V., Zalozniaia, I. V., and Arutjunyan, A. V. (2021) Prenatal hyperhomocysteinemia induces glial activation and alters neuroinflammatory marker expression in infant rat hippocampus, *Cells*, **10**, 1536, https://doi.org/10.3390/cells10061536.
35. Shcherbitskaia, A. D., Vasilev, D. S., Milyutina, Y. P., Tumanova, N. L., Zalozniaia, I. V., Kerkeshko, G. O., and Arutjunyan, A. V. (2020) Maternal hyperhomocysteinemia induces neuroinflammation and neuronal death in the rat offspring cortex, *Neurotox. Res.*, **38**, 408-420, https://doi.org/10.1007/s12640-020-00233-w.
36. Wang, H. L., and Lai, T. W. (2014) Optimization of Evans blue quantitation in limited rat tissue samples, *Sci. Rep.*, **4**, 6588, https://doi.org/10.1038/srep06588.
37. Wick, M. J., Harral, J. W., Loomis, Z. L., and Dempsey, E. C. (2018) An optimized Evans blue protocol to assess vascular leak in the mouse, *J. Vis. Exp.*, **139**, 57037, https://doi.org/10.3791/57037.
38. Dayal, S., and Lentz, S. R. (2008) Murine models of hyperhomocysteinemia and their vascular phenotypes, *Arterioscler. Thromb Vasc. Biol.*, **28**, 1596-1605, https://doi.org/10.1161/ATVBAHA.108.166421.
39. Nieraad, H., Pannwitz, N., Bruin, N., Geisslinger, G., and Till, U. (2021) Hyperhomocysteinemia: metabolic role and animal studies with a focus on cognitive

performance and decline – a review, *Biomolecules*, **11**, 1546, https://doi.org/10.3390/biom11101546.

40. Sauls, D. L., Arnold, E. K., Bell, C. W., Allen, J. C., and Hoffman, M. (2007) Pro-thrombotic and pro-oxidant effects of diet-induced hyperhomocysteinemia, *Thrombosis Res.*, **120**, 117-126, https://doi.org/10.1016/j.thromres.2006.08.001.
41. Ditscheid, B., Funfstuck, R., Busch, M., Schubert, R., Gerth, J., and Jahreis, G. (2005) Effect of L-methionine supplementation on plasma homocysteine and other free amino acids: a placebo-controlled double-blind cross-over study, *Eur. J. Clin. Nutr.*, **59**, 768-775, https://doi.org/10.1038/sj.ejcn.1602138.
42. Andersson, A., Brattstrom, L., Israelsson, B., Isaksson, A., and Hultberg, B. (1990) The effect of excess daily methionine intake on plasma homocysteine after a methionine loading test in humans, *Clin. Chim. Acta*, **192**, 69-76, https://doi.org/10.1016/0009-8981(90)90273-u.
43. Benevenga, N. J., and Steele, R. D. (1984) Adverse effects of excessive consumption of amino acids, *Annu. Rev. Nutr.*, **4**, 157-181, https://doi.org/10.1146/annurev.nu.04.070184.001105.
44. Terstappen, F., Tol, A. J. C., Gremmels, H., Wever, K. E., Paauw, N. D., Joles, J. A., Beek, E. M. V., and Lely, A. T. (2020) Prenatal amino acid supplementation to improve fetal growth: a systematic review and meta-analysis, *Nutrients*, **12**, 2535, https://doi.org/10.3390/nu12092535.
45. Stanescu, S., Belanger-Quintana, A., Fernandez-Felix, B. M., Ruiz-Sala, P., Del Valle, M., Garcia, F., Arrieta, F., and Martinez-Pardo, M. (2022) Interorgan amino acid interchange in propionic acidemia: the missing key to understanding its physiopathology, *Amino Acids*, **54**, 777-786, https://doi.org/10.1007/s00726-022-03128-6.
46. Benevenga, N. J. (1974) Toxicities of methionine and other amino acids, *J. Agric. Food Chem.*, **22**, 2-9, https://doi.org/10.1021/jf60191a036.
47. Cleal, J. K., Lofthouse, E. M., Sengers, B. G., and Lewis, R. M. (2018) A systems perspective on placental amino acid transport, *J. Physiol.*, **596**, 5511-5522, https://doi.org/10.1113/JP274883.
48. McIntyre, K. R., Hayward, C. E., Sibley, C. P., Greenwood, S. L., and Dilworth, M. R. (2019) Evidence of adaptation of maternofetal transport of glutamine relative to placental size in normal mice, and in those with fetal growth restriction, *J. Physiol.*, **597**, 4975-4990, https://doi.org/10.1113/JP278226.
49. Hussain, T., Tan, B., Murtaza, G., Metwally, E., Yang, H., Kalhoro, M. S., Kalhoro, D. H., Chughtai, M. I., and Yin, Y. (2020) Role of dietary amino acids and nutrient sensing system in pregnancy associated disorders, *Front. Pharmacol.*, **11**, 586979, https://doi.org/10.3389/fphar.2020.586979.
50. Huang, H., Vandekeere, S., Kalucka, J., Bierhansl, L., Zecchin, A., Bruning, U., Visnagri, A., Yuldasheva, N., Goveia, J., Cruys, B., Brepoels, K., Wyns, S., Rayport, S., Ghesquiere, B., Vinckier, S., Schoonjans, L., Cubbon, R., Dewerchin, M., Eelen, G., and Carmeliet, P. (2017) Role of glutamine and interlinked asparagine metabolism in vessel formation, *EMBO J.*, **36**, 2334-2352, https://doi.org/10.15252/embj.201695518.
51. Bonnin, A., Goeden, N., Chen, K., Wilson, M. L., King, J., Shih, J. C., Blakely, R. D., Deneris, E. S., and Levitt, P. (2011) A transient placental source of serotonin for the fetal forebrain, *Nature*, **472**, 347-350, https://doi.org/10.1038/nature09972.
52. Bonnin, A., and Levitt, P. (2011) Fetal, maternal, and placental sources of serotonin and new implications for developmental programming of the brain, *Neuroscience*, **197**, 1-7, https://doi.org/10.1016/j.neuroscience.2011.10.005.
53. Mao, J., Jain, A., Denslow, N. D., Nouri, M. Z., Chen, S., Wang, T., Zhu, N., Koh, J., Sarma, S. J., Sumner, B. W., Lei, Z., Sumner, L. W., Bivens, N. J., Roberts, R. M., Tuteja, G., and Rosenfeld, C. S. (2020) Bisphenol A and bisphenol S disruptions of the mouse placenta and potential effects on the placenta-brain axis, *Proc. Natl. Acad. Sci. USA*, **117**, 4642-4652, https://doi.org/10.1073/pnas.1919563117.
54. Woods, L., Perez-Garcia, V., and Hemberger, M. (2018) Regulation of placental development and its impact on fetal growth-new insights from mouse models, *Front. Endocrinol. (Lausanne)*, **9**, 570, https://doi.org/10.3389/fendo.2018.00570.
55. Baskurt, O. K., and Meiselman, H. J. (2012) Iatrogenic hyperviscosity and thrombosis, *Semin. Thromb. Hemost.*, **38**, 854-864, https://doi.org/10.1055/s-0032-1325616.
56. Winterhager, E., and Gellhaus, A. (2017) Transplacental nutrient transport mechanisms of intrauterine growth restriction in rodent models and humans, *Front. Physiol.*, **8**, 951, https://doi.org/10.3389/fphys.2017.00951.
57. Rosario, F. J., Kanai, Y., Powell, T. L., and Jansson, T. (2015) Increased placental nutrient transport in a novel mouse model of maternal obesity with fetal overgrowth, *Obesity (Silver Spring)*, **23**, 1663-1670, https://doi.org/10.1002/oby.21165.
58. Aye, I. L., Rosario, F. J., Powell, T. L., and Jansson, T. (2015) Adiponectin supplementation in pregnant mice prevents the adverse effects of maternal obesity on placental function and fetal growth, *Proc. Natl. Acad. Sci. USA*, **112**, 12858-12863, https://doi.org/10.1073/pnas.1515484112.
59. Huang, Z., Huang, S., Song, T., Yin, Y., and Tan, C. (2021) Placental angiogenesis in mammals: a review of the regulatory effects of signaling pathways and functional nutrients, *Adv. Nutr.*, **12**, 2415-2434, https://doi.org/10.1093/advances/nmab070.
60. Yung, H. W., Hemberger, M., Watson, E. D., Senner, C. E., Jones, C. P., Kaufman, R. J., Charnock-Jones, D. S., and Burton, G. J. (2012) Endoplasmic reticulum stress

disrupts placental morphogenesis: implications for human intrauterine growth restriction, *J. Pathol.*, **228**, 554-564, https://doi.org/10.1002/path.4068.
61. Cross, J. C., Hemberger, M., Lu, Y., Nozaki, T., Whiteley, K., Masutani, M., and Adamson, S. L. (2002) Trophoblast functions, angiogenesis and remodeling of the maternal vasculature in the placenta, *Mol. Cell Endocrinol.*, **187**, 207-212, https://doi.org/10.1016/s0303-7207(01)00703-1.
62. Wang, Y., Engel, T., and Teng, X. (2024) Post-translational regulation of the mTORC1 pathway: a switch that regulates metabolism-related gene expression, *Biochim. Biophys. Acta Gene Regul. Mech.*, **1867**, 195005, https://doi.org/10.1016/j.bbagrm.2024.195005.
63. Kavitha, J. V., Rosario, F. J., Nijland, M. J., McDonald, T. J., Wu, G., Kanai, Y., Powell, T. L., Nathanielsz, P. W., and Jansson, T. (2014) Down-regulation of placental mTOR, insulin/IGF-I signaling, and nutrient transporters in response to maternal nutrient restriction in the baboon, *FASEB J.*, **28**, 1294-1305, https://doi.org/10.1096/fj.13-242271.
64. Qin, X., Jiang, B., and Zhang, Y. (2016) 4E-BP1, a multifactor regulated multifunctional protein, *Cell Cycle*, **15**, 781-786, https://doi.org/10.1080/15384101.2016.1151581.
65. Pang, V., Bates, D. O., and Leach, L. (2017) Regulation of human feto-placental endothelial barrier integrity by vascular endothelial growth factors: competitive interplay between VEGF-A(165)a, VEGF-A(165)b, PIGF and VE-cadherin, *Clin. Sci. (Lond)*, **131**, 2763-2775, https://doi.org/10.1042/CS20171252.
66. Saunders, N. R., Dziegielewska, K. M., Mollgard, K., and Habgood, M. D. (2015) Markers for blood-brain barrier integrity: how appropriate is Evans blue in the twenty-first century and what are the alternatives? *Front. Neurosci.*, **9**, 385, https://doi.org/10.3389/fnins.2015.00385.
67. Haghighi Poodeh, S., Salonurmi, T., Nagy, I., Koivunen, P., Vuoristo, J., Rasanen, J., Sormunen, R., Vainio, S., and Savolainen, M. J. (2012) Alcohol-induced premature permeability in mouse placenta-yolk sac barriers *in vivo*, *Placenta*, **33**, 866-873, https://doi.org/10.1016/j.placenta.2012.07.008.
68. Lewis, R. M., Baskaran, H., Green, J., Tashev, S., Palaiologou, E., Lofthouse, E. M., Cleal, J. K., Page, A., Chatelet, D. S., Goggin, P., and Sengers, B. G. (2022) 3D visualization of trans-syncytial nanopores provides a pathway for paracellular diffusion across the human placental syncytiotrophoblast, *iScience*, **25**, 105453, https://doi.org/10.1016/j.isci.2022.105453.
69. Sibley, C. P., Brownbill, P., Glazier, J. D., and Greenwood, S. L. (2018) Knowledge needed about the exchange physiology of the placenta, *Placenta*, **64**, S9-S15, https://doi.org/10.1016/j.placenta.2018.01.006.
70. Shao, X., Cao, G., Chen, D., Liu, J., Yu, B., Liu, M., Li, Y. X., Cao, B., Sadovsky, Y., and Wang, Y. L. (2021) Placental trophoblast syncytialization potentiates macropinocytosis via mTOR signaling to adapt to reduced amino acid supply, *Proc. Natl. Acad. Sci. USA*, **118**, e2017092118, https://doi.org/10.1073/pnas.2017092118.
71. Cooke, L. D. F., Tumbarello, D. A., Harvey, N. C., Sethi, J. K., Lewis, R. M., and Cleal, J. K. (2021) Endocytosis in the placenta: an undervalued mediator of placental transfer, *Placenta*, **113**, 67-73, https://doi.org/10.1016/j.placenta.2021.04.014.
72. Elshorbagy, A. K., Graham, I., and Refsum, H. (2020) Body mass index determines the response of plasma sulfur amino acids to methionine loading, *Biochimie*, **173**, 107-113, https://doi.org/10.1016/j.biochi.2020.03.001.
73. Lofthouse, E. M., Manousopoulou, A., Cleal, J. K., O'Kelly, I. M., Poore, K. R., Garbis, S. D., and Lewis, R. M. (2021) N-acetylcysteine, xCT and suppression of Maxi-chloride channel activity in human placenta, *Placenta*, **110**, 46-55, https://doi.org/10.1016/j.placenta.2021.05.009.
74. Da Silva, V. C., Fernandes, L., Haseyama, E. J., Agamme, A. L., Guerra Shinohara, E. M., Muniz, M. T., and D'Almeida, V. (2014) Effect of vitamin B deprivation during pregnancy and lactation on homocysteine metabolism and related metabolites in brain and plasma of mice offspring, *PLoS One*, **9**, e92683, https://doi.org/10.1371/journal.pone.0092683.